Thin Film Transmission Matrix Approach to Fourier Transform Infrared Analysis of HgCdTe Multilayer Heterostructures

D.D. LOFGREEN,[1,2] C.M. PETERSON,[1] A.A. BUELL,[1] M.F. VILELA,[1] and S.M. JOHNSON[1]

1.—Raytheon Vision Systems, Goleta, CA 93117. 2.—E-mail: daniel_d_lofgreen@raytheon.com

The ability to achieve high-yield focal plane arrays from $Hg_{1-x}Cd_xTe$ molecular beam epitaxy material depends strongly on postgrowth wafer analysis. Nondestructive analysis that can determine layer thicknesses as well as alloy compositions is critical in providing run-to-run consistency. In this paper, we incorporate the use of a thin film transmission matrix model to analyze Fourier transform infrared (FTIR) transmission spectra. Our model uses a genetic algorithm along with a multidimensional, nonlinear minimization Nelder–Mead algorithm to determine the composition and thickness of each layer in the measured epitaxial structure. Once a solution has been found, the software is able to predict detector performance such as quantum efficiency and spectral response. We have verified our model by comparing detector spectral data to our predicted spectral data derived from the room-temperature FTIR transmission data. Furthermore, the model can be used to generate design curves for detectors with varying absorber thicknesses and/or different operating temperatures. The consequence of this are reduced cycle times and reduced design variations.

Key words: $Hg_{1-x}Cd_xTe$ (MCT), Fourier transform infrared spectroscopy (FTIR), transmission matrix, refractive index, bandgap

INTRODUCTION

Predicting $Hg_{1-x}Cd_xTe$ (MCT) detector performance grown by molecular beam epitaxy (MBE) using nondestructive, postgrowth wafer analysis is quickly becoming commonplace in the focal plane array (FPA) industry.[1,2] The ability to screen wafers prior to processing allows for the selection of those wafers that are most likely to pass specification. The result of this is increased yield and reduced costs. Furthermore, this analysis can be used as feedback to the MBE process itself, again improving yield. Quick and accurate feedback is therefore essential in providing run-to-run consistency.

The most common form of postgrowth analysis is Fourier transform infrared (FTIR) spectroscopy. Traditionally, FTIR data are analyzed by taking the Fourier transform of the transmission spectra and looking for peaks.[3] This technique is greatly complicated when the structure being analyzed has layers of different refractive indices and thicknesses. In fact, this technique can really be used effectively only to determine the average composition and total layer thickness. Analyzing two-color detector structures, where information regarding both bands is desired, becomes complicated, and neither individual layer thickness nor composition can be effectively filtered out.[4] Furthermore, if the structure contains layers that are optically thin with respect to the wavelength of light being used to measure the transmission, the accuracy is greatly diminished.

These deficiencies in analyzing the data can be overcome by modeling the FTIR transmission using the transmission matrix formalism outlined by Yeh.[5] For this technique to work properly, very accurate expressions for the complex dielectric function must be known. This means that we need an accurate model not only for the real part of the refractive index, but also for the bandgap, absorption coefficient, and below band absorption, all of which must be self consistent through the composition of the material. The desired layer compositions and thicknesses can then be determined by solving the model using a genetic algorithm[6] along with a multidimensional, nonlinear minimization Nelder–Mead algorithm,[7] with the figure of merit being an overlap integral that will be described later.

(Received November 7, 2005; accepted January 30, 2006)

To maintain computational efficiency, the real part of the dielectric function was taken from the literature. Because we were mostly interested in middle wave (MW) and long wave (LW) detectors, we chose to use the Sellmeier equation for the refractive index of MCT given by Kucera,[8] the expression for CdTe given by Marple,[9] and the expression for ZnTe given by Jensen.[10] To handle the refractive index dispersion as the energy approaches the bandgap, the value of the index was held constant at a value equal to that just below the bandgap. For the imaginary part of the dielectric function, we chose to use a standard Urbach band tail that was calibrated for various MCT compositions and temperatures[11] along with absorption model proposed by Moazzami[12] based on the hyperbolic band structure for MCT.[13]

More importantly was the model for the bandgap of MCT. Initially we started with the Hansen, Schmidt, and Casselman (HSC) model.[14] However, as the experimental data will show, it was necessary to alter this model to fit our data.

EXPERIMENTAL RESULTS

To test the model, single composition layers were grown by MBE. These layers where characterized by secondary ion mass spectroscopy (SIMS) and scanning electron microscopy (SEM). Through SEM, the thickness of the layer could be accurately determined, and from SIMS, the uniformity of the composition was verified. After measurement by FTIR at 300 K, the composition and thickness were determined by solving the model. The sample was then placed inside a cold finger and FTIR measurements were taken at 78 K using a Perkin Elmer (Wellesley, MA) Lambda-983G spectrometer. Using the composition and thickness values from the model at 300 K, the temperature in the model was simply changed to 78 K, and the results were compared to the measured data. What we found was that using the HSC model for bandgap did not accurately represent the FTIR data at 78 K. A new model for bandgap of MCT was then proposed that was valid over the range $0.20 < x < 0.35$ and for temperatures $78\ K < T < 300\ K$.

$$E_g = (Ax + B)T + (Cx + D) \tag{1}$$

$$A = -1.6618 \times 10^{-3} \quad C = 1.88591$$
$$B = 7.4564 \times 10^{-4} \quad D = -0.34919$$

Using the expression for bandgap in Eq.(1), we were able to use our model to determine composition and thickness for single layers while being self-consistent at both 300 K and 78 K. The comparison of the measured data to the model using the HSC bandgap and the RVS bandgap for two different compositions is shown in Fig. 1. The difference between these two models is highlighted in Table I. The most obvious difference between the models is the bandgap for compositions $x < 0.30$ at 78 K. In fact, without the new bandgap model in Eq. 1, we were unable to accurately predict long-wave infrared (LWIR) detector performance.

As structures become more complicated with hetero interfaces, multiple absorber regions, and possible graded compositions, so does the parameter space for the solution. A genetic algorithm is used to find the right starting point for all the free variables. Once the best initial condition has been found, the Nelder–Mead algorithm is used to find the optimal solution. The figure of merit used to find the solution is an overlap integral:

$$\Phi = \frac{\int \Psi_1^* \Psi_2 d\lambda}{\int |\Psi_1|^2 d\lambda \int |\Psi_2|^2 d\lambda} \tag{2}$$

Ψ_1 is the measured transmission and Ψ_2 is the modeled transmission. As the model approaches the measured data, Φ approaches 1. Once the optimal solution is found, the modeled structure is transformed to 78 K.

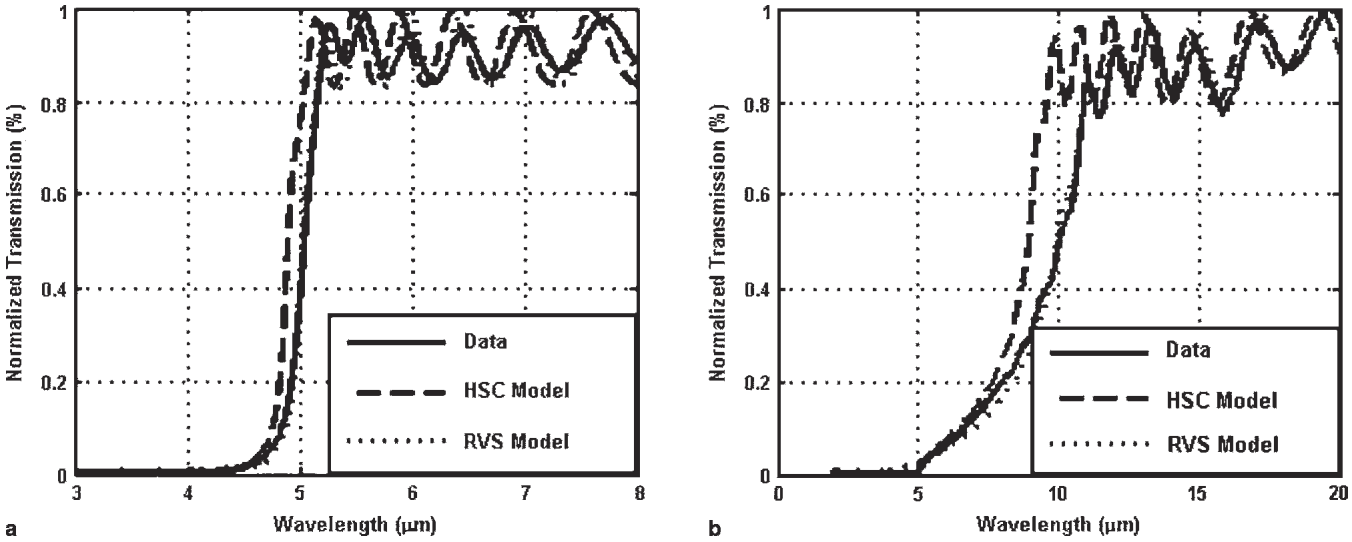

Fig. 1. Normalized FTIR transmission data at 78K compared to the model using the HSC bandgap and the RVS bandgap for (a) a nominal MWIR layer and (b) a nominal LWIR layer.

Table I. Comparison of Band Gap, E_g, between Hansen et al. (HSC) and Our Model (RVS)

x Value	E_g (eV) HSC (300 K)	E_g (eV) RVS (300 K)	ΔE_g (eV) (300 K)	E_g (eV) HSC (78 K)	E_g (eV) RVS (78 K)	ΔE_g (eV) (78 K)
0.20	0.1546	0.1520	0.0026	0.0833	0.0602	0.0231
0.25	0.2231	0.2213	0.0018	0.1637	0.1480	0.0157
0.30	0.2908	0.2907	0.0001	0.2433	0.2359	0.0074
0.35	0.3581	0.3601	−0.0020	0.3225	0.3237	−0.0012
0.40	0.4257	0.4295	−0.0037	0.4020	0.4115	−0.0095

Then, very simple models can be used to predict quantum efficiency, η, and responsivity, R.

$$\eta = 1 - T(x, \lambda, T) \tag{3}$$

$$R = \frac{\lambda \eta}{hc} q \tag{4}$$

The first T in the quantum efficiency expression is transmission, and the second T is temperature.

Accuracy of the Multilayer Heterostructure Model

The transmission matrix model was first put to the test by modeling LWIR detectors detector structures grown on silicon.[15] In the case of a LWIR on Si detector, the model must determine all the pertinent compositions and thicknesses in the MCT as well as the thickness of the CdTe/ZnTe buffer. After detectors are fabricated, the normalized response per photon can be compared to the prediction. It is important to keep accurate data regarding the location of the measured detector on the wafer, for slight nonuniformity can shift the detector cutoff. The data can then be compared to the FTIR data taken at the same location. Figure 2 shows the results of the model compared to prediction.

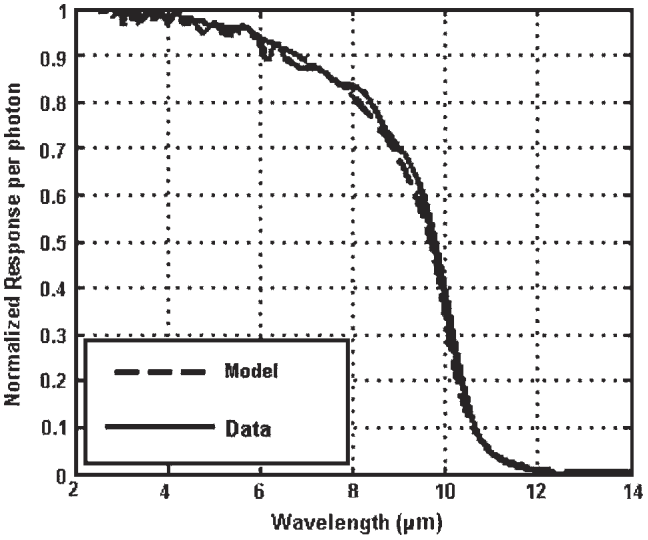

Fig. 2. Modeled response per photon of a LWIR detector on Si compared to measured data.

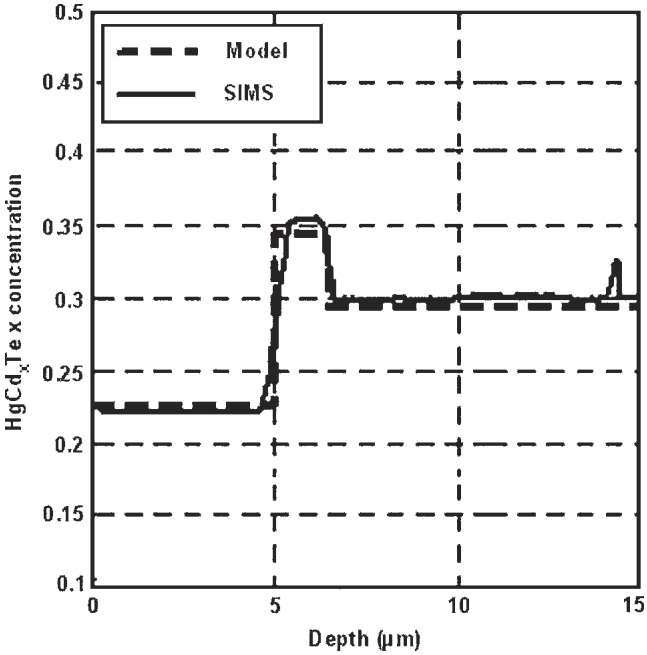

Fig. 3. Modeled layer composition for a MWIR/LWIR two color detector structure compared to SIMS profile.

Based on the excellent results shown in Fig. 2, the model was then extended to predict two-color detector structures grown by MBE.[16] The model was first verified by comparing the modeled results to SIMS analysis. The results of this are shown in Fig. 3. From the plots in the figure, it is clear that the model was able to accurately determine the composition and thickness of each absorber band. From the figure it can be seen that there are slight grades at the heterointerfaces. While these grades can be included into the model as piecewise steps, their addition adds very little as far as being able to predict detector response. With the proper structure modeled, we were then able to predict the response from each band.

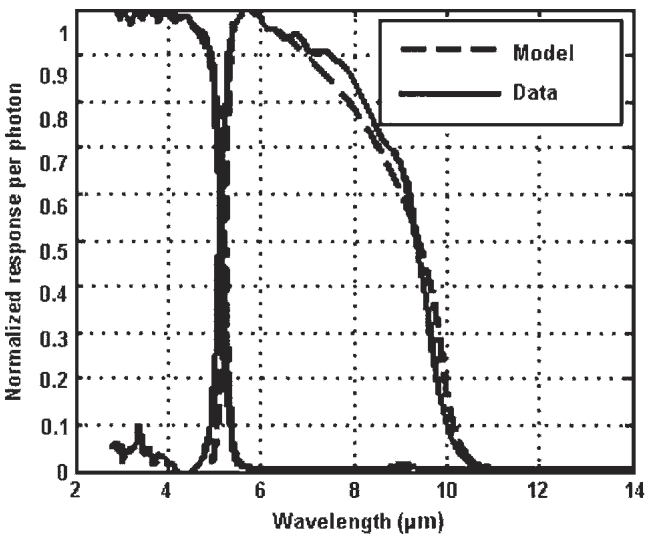

Fig. 4. Modeled 78 K response per photon of a MWIR/LWIR two color detector compared to measured data.

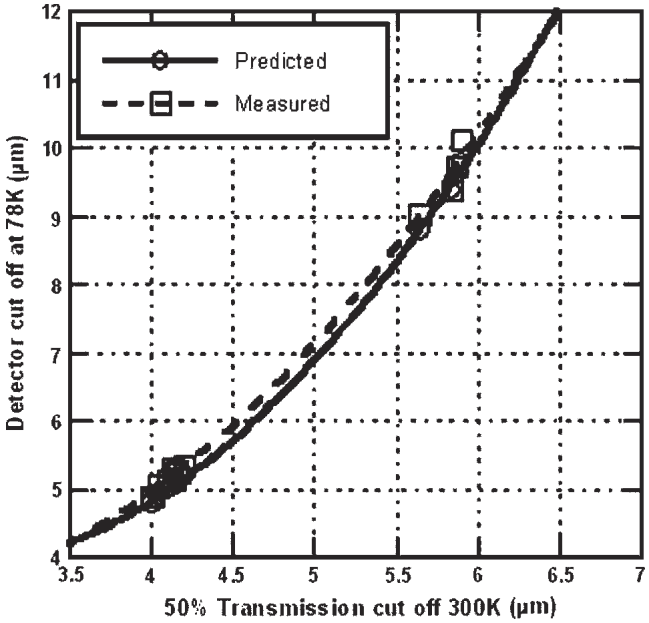

Fig. 5. Predicted and measured detector cutoff values at 78 K vs. the 50% transmission cutoff point at room temperature.

The modeled 78 K detector response for both the middle wave infrared (MWIR) and LWIR bands of a two color detector structure compared to the measured data are shown in Fig. 4. While the model does an excellent job predicting detector cutoff, the shape of the response is not perfect. We surmise that there is reflection from the top contact of the LW band, which adds to absorption near the band edge that is not included in the model. These reflections could be added to the model; however, they could not be compared to the transmission measurement. Nevertheless, as a predictive model used to screen wafers, this method has proved very accurate.

By collecting detector spectral data along with FTIR transmission data, a set of detector cutoff values can be plotted against the predicted cutoff values from the model. The result of this analysis is shown in Fig. 5. From this figure, one can see how accurately this model can predict detector performance over a wide range of cutoff values. Furthermore, we can now use this model to generate design curves for detectors with varying absorber thicknesses and/or different operating temperatures. The consequence of this being reduced cycle times and reduced design variations.

CONCLUSIONS

We have demonstrated a fast, accurate, and robust method for analyzing FTIR data from multilayer MCT structures grown by MBE. The model is useful over a wide range of compositions and can be extended further if needed. The model has been able to accurately predict individual layer thicknesses as well as compositions. This was made possible by developing a new bandgap model from our measured data. This model has been compared to the classic HSC model, and findings showed that it varies only slightly at low x-value compositions.

It was important to verify the accuracy of our model, especially when it came to the determination of multicolor structures. We were able to verify the thickness and composition accuracy using SIMS and SEM analysis. We further verified the model by accurately predicting detector response from MWIR, LWIR, and M/L two-color detector structures.

Due to the nature of the optimization algorithm, the solution convergence time is very fast. Therefore, this analysis technique is now used to scan the entire wafer prior to processing. This provides constant feedback to the growth process and allows us to screen wafers. Knowledge of the layer thicknesses and compositions allow for better run-to-run reproducibility and to higher yields.

ACKNOWLEDGEMENTS

This work was funded by Raytheon IR&D. We could also like to thank John Roth and Brett Nosho at HRL Laboratories, LLC for some of the data collection and discussions.

REFERENCES

1. M. Daraselia, M. Carmody, M. Zandian, and J.M. Arias, *J. Electron. Mater.* 33, 761 (2004).
2. M. Daraselia, M. Carmody, D.D. Edwall, and T.E. Tiwald, *J. Electron. Mater.* 34, 762 (2005).
3. P.R. Griffiths and J.A. De Haseth, *Fourier Transform Infrared Spectrometry* (New York: Wiley, 1986).
4. V. Ariel, V. Garber, G. Bahir, S. Krishnamurthy, and A. Sher, *Appl. Phys. Lett.* 69, 1864 (1996).
5. P. Yeh, *Optical Waves in Layered Media* (New York: Wiley, (1988).
6. D. Goldberg, *Genetic Algorithms* (Reading, MA: Addison-Wesley, 1989).
7. J.A. Nelder and R. Mead, *Computer J.* 7, 308 (1965).
8. Z. Kucera, *Phys. Status Solidi A* 100, 659 (1987).
9. D.T.F. Marple, *J. Appl. Phys.* 35, 539 (1964).
10. B. Jensen and A. Torabi, *J. Appl. Phys.* 54, 2030 (1983).
11. E. Finkman and S.E. Schacham, *J. Appl. Phys.* 56, 2896 (1984).
12. K. Moazzami, J. Phillips, D. Lee, D. Edwall, M. Carmody, E. Piquette, M. Zandian, and J. Arias, *J. Electron. Mater.* 33, 701 (2004).
13. S. Krishnamurthy, A.B. Chen, and A. Sher, *J. Appl. Phys.* 80, 4045 (1996).
14. G.L. Hansen, J.L. Schmidt, and T.N. Casselman, *J. Appl. Phys.* 53, 7099 (1982).
15. S.M. Johnson et al, *J. Electron. Mater.* 33, 526 (2004).
16. E.P.G. Smith et al, *J. Electron. Mater.* 33, 509 (2004).